Chapter

Medical Application of Ultra-Wideband Technology

Abdulhameed Habeeb Alghanimi

Abstract

This chapter deals with the applications of ultra-wideband technology, especially for medical scope, and the most features and advantages that made it useful in this scope. Also, the chapter has been included with the most important medical applications of UWB technology. Ultra-wideband radar for angiography and UWB glucometer are the main applications which will be explained in this chapter. The exposure for safety aspects, the dielectric properties of human tissues, blood dielectric properties measurement using open-ended coaxial probe experiment to improve the blood image, and the ideal ultra-wideband pulses' shape, width, and repetition time that are used for medical applications have been illustrated. Finally, the results (figures, tables, and experiment results), conclusions, and discussions have been mentioned.

Keywords: UWB medical application, UWB medical radar, UWB glucometer, UWB features, UWB exposure safety aspects

1. Introduction

UWB is an emerging wireless communication technology that introduces a wide approach of wireless techniques in various disciplines, especially in medical applications. This technology works with a frequency range of 3.1–10.6 GHz and power spectrum density (PSD) of −41.3 dBm/MHz according to the American Federal Communications Commission (FCC) as depicted in **Figure 1** [1] and International Commission on Non-Ionizing Radiation Protection (ICNIRP) safety guidelines [2]. This frequency range with low-power consumption makes the technology suitable for use in medical applications. It has no biological side effects and has nonionizing radiation (only thermal effect) as well as it has a good ability to penetrate the human tissues. These features encourage the researchers to propose many studies that have invested UWB in medical applications; most of these papers would focus either on the differences in the dielectric properties of human tissue like breast cancer detection, or on the organ movement detection like heart rate and respiratory detection. The main problems that have been faced by such researches are the absorption and attenuation of the signal by the skin and the vicinity layers, while the returning signal from the deep layers is very weak, as well as the inability to distinguish between the tissues that have convergent dielectric properties. These problems will introduce new challenges to be solved by researchers.

1.1 UWB advantages and features in medical application

- Good ability of penetration for human tissue.

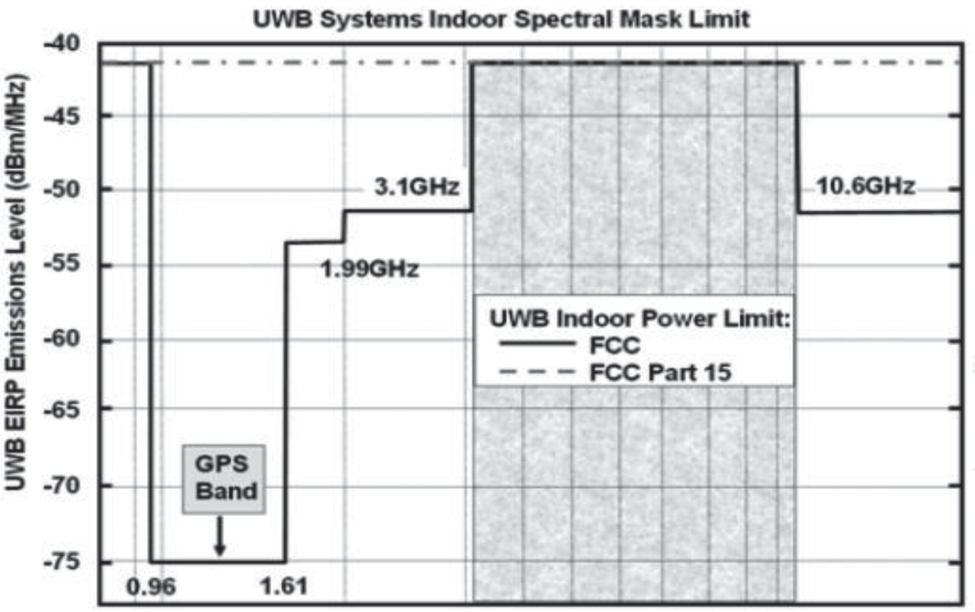

Figure 1.
Indoor power spectrum mask from FCC [1].

- Selective addressing (multiuser).
- High capacity of channel.
- Low cost, low-power consumption, and low complexity.
- Noise-like signal.
- Low probability of interception, jamming, and resistive to a multipath problem.
- High resolution in the time domain making UWB used for location and tracking applications.
- Do not have any biological side effects on the human tissue (low power and nonionizing).

1.2 UWB monocycle pulses

UWB medical radar naturally deals with human body tissues, which will absorb and affect on the radiated energy of UWB pulses, so we have a challenge with increasing the radiated energy without crossing the FCC mask [1], which depends on the Gaussian pulse shape (derivative order), width, and repetition time (frequency). Here, the first derivative of Gaussian pulse equation is:

$$\mathbf{Gs}(\mathbf{t}) = \mathbf{A}\ \exp\left[-\left(\frac{t}{\mathfrak{G}}\right)^2\right] \tag{1}$$

and the fifth derivative of Gaussian pulses is as the following as in Eq. (2), and the frequency range of indoor application from 4 to 6 GHz introduces the best performance and best masking to FCC [1, 3]:

$$\mathbf{Gs}(\mathbf{t}) = \mathrm{A}\left(-\frac{t^5}{\sqrt{2\pi}\mathfrak{G}^{11}} + \frac{10t^3}{\sqrt{2\pi}\mathfrak{G}^{9}} + \frac{15t}{\sqrt{2\pi}\mathfrak{G}^{7}}\right)\exp\left(-\frac{t^2}{2\mathfrak{G}^2}\right) \tag{2}$$

where A is the pulse amplitude, t is time, and ꚍ is a time constant as illustrated in **Figure 2** [4]. So, it has safe electromagnetic field according to FCC and the *International Commission on Non-Ionizing Radiation Protection (*ICNIRP) guidelines and it may be causing thermal effects related to the power absorption by human tissue [1, 2, 5].

1.3 The dielectric properties

The dielectric properties are the fundamental parameters that affect the propagation of the electric field. It is a measure of how electric field behaves or interacts with materials, which can be used (for example) to understand how easily an electric field will polarize a given dielectric material. Dielectric constant and loss tangent are both numerical values using which permittivity of a dielectric material can be defined. And the conductivity is the extent of electric current that flow through it. Where the conductivity is used for the rate or degree that electromagnetic wave, electricity, heat, or sound travel through a certain medium.

The dielectric properties of blood have been affected by many coefficients like blood temperature [6], applied electromagnetic wave frequency, clotting rate, human gender [7], blood group type (A, B, AB, and O) [8], blood composition, blood hematocrit level, and hemoglobin percentage [9].

1.4 Blood dielectric properties measurement using open-ended coaxial probe

The dielectric properties will be different from one material to another where these differences will enable the recognizing of the tissues by recognizing its dielectric properties [10]. This experiment attempts to improve the blood dielectric properties individually for increasing the blood appearing over other substances (perfect blood image). This microwave measurement method (experiment) has been applied in 5 GHz frequency center and in a temperature of 37°C; the blood samples with different additions and concentrations have been tested and the results have been recorded. The required experiment devices are shown in **Figure 3**.

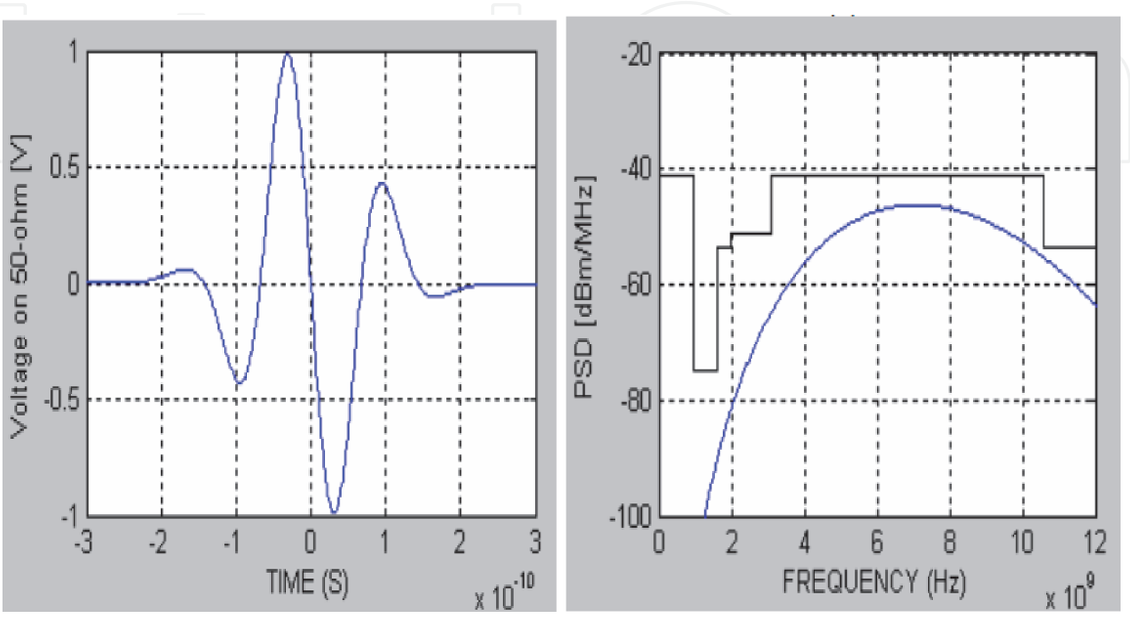

Figure 2.
Fifth derivative Gaussian pulse [4].

The measurement system has the following components:

- RF vector network analyzer (compatible with the above probe model: E5063A ENA series).
- Open-ended coaxial probe (model: 85070E performance probe).
- Water bath and thermistor.
- Adjustable probe stand.
- PC computer (laptop).
- Glass sample containers and alcohol wipes.

The permittivity equation will be as follow [11]:

$$\varepsilon = \frac{2\Gamma \sin\left[2s + \frac{2\pi(L_2 - L_1)}{\lambda}\right.}{s\left\{1 + \Gamma^2 + 2\Gamma \cos\left[2s + \frac{2\pi(L_2 - L_1)}{\lambda}\right]\right)} \quad (3)$$

where λ is the wavelength, Γ is the reflection coefficient, and s is standing wave ratio.

1.5 Safety aspects for the human tissue that exposed to UWB

The use of UWB electromagnetic wave spectrum in medical application that penetrates human body tissue makes a challenge with the patient safety (safe exposure). On the other hand, because its band is 3.1–10.6 GHz, the major effects of UWB using on the human tissue are the thermal effects. These effects are caused by

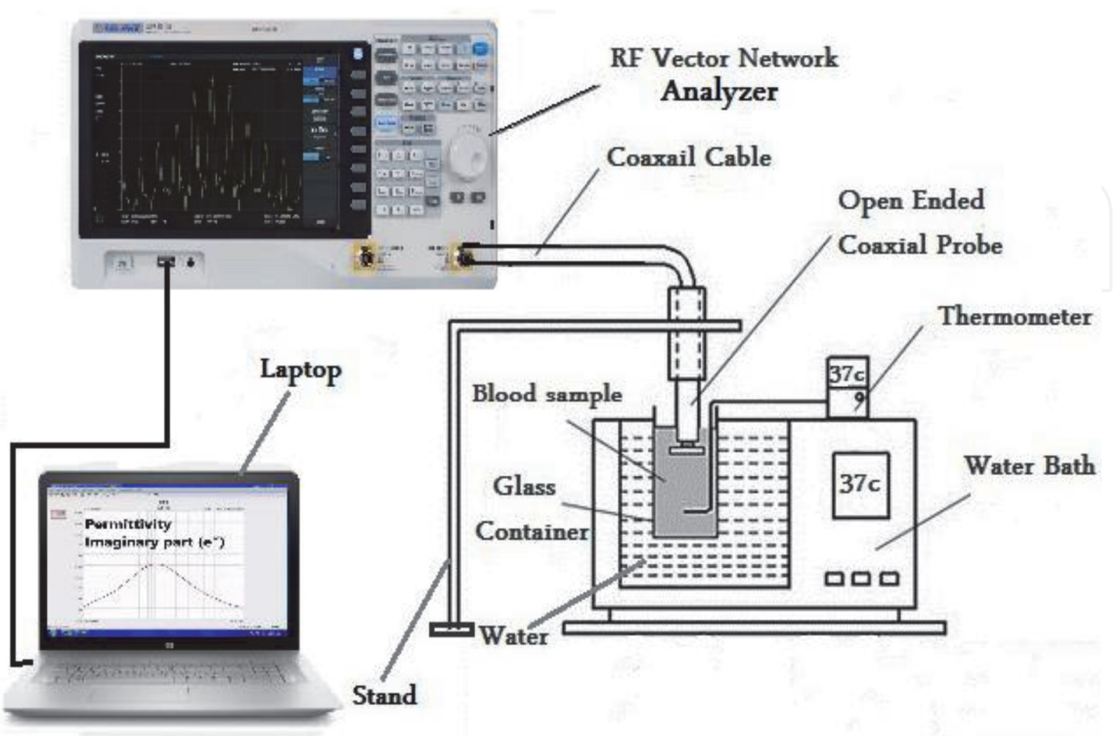

Figure 3.
Blood dielectric properties measurement system.

power absorption and related to the specific absorption rate (SAR) [12], which is measured by W/kg. The available research indicates an increase in the SAR level of whole body equals to 1 and 4 W/kg when it exposes to an electromagnetic field up to 100 kHz for about 30 min, and this increase in SAR causes an increase in the temperature of body less than 1°C [2]. Also, the animal data prove that if the SAR level is raised over than 4 W/kg, it can be out of body control and cause harmful effects of tissue heating, while epidemiological surveys are showing that no biological effects are indicated on workers or the public in the same environment [2].

The SAR level is limited by ICNIRP [2] and FCC [1]. The basic restrictions' limitation is 0.4 W/kg for the worker, 10 W/kg averaged over 10 g mass for head and spinal zones, and 0.08 W/kg for the public population. Moreover, "although little information is available on the relation between biological effects and peak values of pulsed fields, it is suggested that for frequencies exceeding 10 MHz, the power density as averaged over the pulse width should not exceed 1000 times the reference levels or that field strengths should not exceed 32 times the field strength reference levels" [13].

2. UWB medical application

Many papers have been published by many researchers and organizations that have proposed ultra-wideband for medical applications, with different frequencies and hypothesis like:

- Breast tumor detection.
- Bone cancer detection.
- Brain hemorrhage detection.
- Position and localization.
- Noncontacting medical imaging.
- Heartbeat and lung movement detection.
- Detection of vascular pressure.
- Vital sign monitoring.
- MRI image improvement.
- Heart volume detection.
- Ultra-wideband radar for angiography.
- Blood glucose concentration level measurement.

Some of these researches are mentioned below:

In 2002, Staderini [14] presented biomedical applications of UWB radar as a mix of ordinary radar (ranging and detection) with spread spectrum radio which combines the two technologies. The paper talked the problem and interaction of radar wave energy with human tissues, and also the motion of internal organs of body and

noncontact probe. The flaw of this paper is the use of 1500 MHz frequency, which is out of the UWB range (3.1–10.6 GHz). So, the results were not intrinsically right.

In 2005, Paulson et al. [15] introduced an overview about the ability of UWB sensor to monitor the internal organs, sense the respiratory, and detect the cardiac function. The noncontacting image with a micro-power impulse remote sensing and low complexity has been introduced, with examples for applying UWB in medical applications. The drawback of this paper is the use of 2 GHz frequency, which is also out of the UWB range (3.1–10.6 GHz). So, the results were not intrinsically right.

In 2007, Staderini et al. [16] proposed an optimal pulsed UWB medical radar for heart beat detection, by detecting the tracking of heart wall movement depending on the obtained pulse echo average and power, which can be obtained by determining the sampling frequency and required acquisition time. The neglecting of the attenuation coefficient of medium of active path in the calculation of this paper represents a drawback.

In 2009, Leib et al. [17] proposed a pulse-based compact UWB radar used for medical diagnostic, focusing on system architecture, correlation receiver, and time delay adjustment; it is also used for detecting heart beat and respiratory movement. This study supposed that the heart beat and respiratory rates have been fixed, while these ranges have discontinuity. This discontinuity caused a high attenuation in the transmitted signal, causing inaccurate readings.

In 2010, Lazaro et al. [18] estimated vital signs monitor that uses an impulse radio UWB radar; the analytical design has been developed for performing the spectral analysis according to the harmonic and intermodulation addressing for respiration and heart signal, with its simulation and proposed harmonic filter. Finally, the results have been introduced to illustrate the accuracy of the technique for heart rate and respiration detection. The flaw of this study is that the detection is difficult if the frequencies of first breath harmonics and heart signal are being closely.

In 2010, Thiel et al. [19] introduced a UWB sensor to improve the magnetic resonance imaging (MRI) especially for cardiovascular and cancer diagnostic. Their study attempted to prove the benefit of motion tracking for high-resolution brain imaging and navigation used with cardiac MRI, and also served to support electrocardiograph (ECG) analyzing. The proposed device worked only with high or ultra-high MRI field and did not benefit with the low-field MRI.

In 2010, Elmissaoui et al. [20] introduced an imaging radar for human tissue by analyzing the return echoes from the body layers. Their research aimed to find the time of arrival (TOA) and electromagnetic propagation direction (Θ) that basically depends on the characteristic properties of human tissue (layers). The study depended on the reflection echoes to form an image, where the echoes from the deep layers are very weak and difficult to detect because of the attenuation (drawback).

In 2011, Jalilvand et al. [21] examined a UWB system to detect a hemorrhagic stroke in a 3D simulated head model, that estimated four layers model and proving that UWB technique is suited for stroke detection, comparing with other medical imaging devices like MRI, CT scan and mammography. This manner introduced an inaccurate stroke image with low resolution which is considered as main drawback.

In 2012, Urdaneta and Wahid [22] studied a UWB imaging to detect the bone cancer. The main feature of this study is the use of monopole antenna in the frequency range 1–10 GHz based on image reconstruction technique. This measures the change between the dielectric properties of bone tissues and tumor by determining the reflection coefficient, and with a certain algorithm, but still with inaccurate size detection and with long calculation time.

In 2016, Ali et al. [23] designed a noninvasive UWB system for reliable glucose concentration level measurement in human blood depending on artificial intelligence, without taking blood sample, by using two UWB micro-strip antennas with signal acquisition and data processing, where the system works in an artificial neural network manner. The system sends the UWB wave in the central frequency of 4.7 GHz from one side and receives it from the other side, and then applying artificial neural network on the received signal, the drawback of this system is the inaccurate readings and the system needs a long training time.

In 2016, Seguin et al. [24] evaluated a UWB transmission signal to detect heart volume changes with frequency range 1.5–4 GHz, depending on the attenuation changes between blood and other tissues, and using TOA determination for each path of UWB, the drawback of this research is its use of only semi-dynamic heart model in the thorax area, also the propagation, and reflection of other layer.

In 2016, Mackenberg et al. [25] attempted to establish a UWB system that detects the vascular pressure based on the detection of vascular dilation inside an inhomogeneous tissue. The researchers found a correlation relationship between the major peaks of signal in time domain and the amplitude of supposed values. These peaks represent the reflection from the boundary layers of proposed phantom depending on the relative and propagation times. The drawback of this study is that all experiments were applied for homogenous tissue and with one layer (silicon), while the real study must be with multilayer. These layers increased the number of reflected signals due to increasing the complexity of measurements.

In 2017, Wang et al. [26] used impulse-radio (IR) UWB sensor for accurately measuring the chest compression depth. This study uses many trails, which are then compared between them. This study did not respect the human body permittivity which has an effect on the calculation of time of arrival (TOA), and it requires heavy instruments in developmental prototype.

In 2018, Alhawari [27] presented lung tumor detection using UWB (microwave imaging approach) that uses microstrip antenna with frequency range 3–4 GHz with best distance of 10 mm far from the thorax. This introduces a radar with the ability of tumor detection of 4 mm diameter in size, which is very accurate comparing with another chest imaging device like ultrasound and X-ray, and with low cost. The used technique is based on the comparison of the dielectric properties of normal tissue and cancerous tissue, where the cancerous tissue has higher dielectric properties than the normal tissue. The drawback of this research is that the blood and muscle tissues have high dielectric properties compared to lung tissue. Also, the experiment needs accurate adjustment for successive examination and the cancerous tissue has different dielectric properties from one case to another.

In 2018, Der et al. [28] produced a UWB radar based on microwave technique with oblique projection and Rao detectors combination to detect breast tumor. This technique is used for reducing the cumbersome clutter and detecting the existence of a tumor, where the tumor region denotes the maximum power; the drawback of this manner is that it is not quite distinguishable in the low signal-to-noise ratio (SNR) case.

In 2018, Selvaraj et al. [29] proposed an UWB antenna and microwave scattering for early breast tissue tumor detection and localization and finding the depth of tumor with frequency range 2.4–4.7 GHz. The study is based on the reflected signal which is received at a microstrip antenna. The signal passed through tumor is attenuated more than the surround normal tissue. This proposed antenna is inactive when the tissue under test is a heterogeneous material.

In 2018, Aziz et al. [30] introduced a graphene-based conductor UWB patch antenna to detect brain tumor. This antenna is operated at a frequency range of 3.15–9.15 GHz depending on the changes between high-reflection coefficient of

normal tissue and low-reflection coefficient of cancerous tissue, as well as based on varying the ground patch width with respect to the value of SAR caused radiation. It is also noted that the antenna length will have an effect on the bandwidth produced, where the length be 7 mm and the antenna is operated as narrowband.

In 2018, Wang [31] proposed an electromagnetic imaging for brain stroke detection based on the changes in the electrical impedance of human tissue in frequency 1–4 GHz with the use of scattered signal to produce a microwave image (MI). The main drawback is that when the stroke is near the skull, it causes an increase in the skull-induced distortion and the system is complicated multi-input multi-output (MIMO).

In 2018, Lee et al. [32] used an IR-UWB radar for monitoring heart rate and rhythms (noncontact). Also, their result's reliability and validity with ordinary ECG are compared. The percentage of mean error is 2.3% vs. 0.2% of normal ECG, which means the UWB radar is inaccurate comparing with the normal ECG. The researchers used MATLAB program to synchronize and store radar readings with normal ECG readings.

In 2018, Shen [33] used a IR-UWB radar to measure the respiration and heart beat rate. The study is based on the autocorrelation, that is, applying fast Fourier transform (FFT) to obtain the respiration rate easily, while reapplying the autocorrelation method after dividing the received signal to the sets of bins and removing one block is the resulting the heartbeat rate signal detection, where the pleural periodical movement caused by the periodicity is displayed as a drawback.

In 2019, Shyu et al. [34] proposed a UWB radar sensor to detect breathing and heart rate. They used First valley peak of the energy function of intrinsic mode functions (FVPIEF) based two-layer ensemble empirical mode decomposition (EEMD). This technique serves the feature time index to detect the frequency of heart beat rate equal to about 1 Hz, which is affected by separating the heart rate from the large breath rate (respiratory). The drawback of this technique is that the breathing movement always masks off the heart beat rate and it is still hidden in the large harmonics and noise.

In 2019, Alghanimi et al. [35] proposed noninvasive blood glucose measurement depending on the relatively changing in the blood dielectric properties by using one ultra-wideband transceiver with a frequency range of 5GHZ and calculating the reflection coefficient through the comparison between the transmitted and reflected signals; the drawback of this study is that there are many factors that can have an effect on the readings of that device like body temperature, gender, blood group, and others.

In 2020, Alghanimi et al. [36] proposed an ultra-wideband radar for angiography by using two different types of antennas. The first antenna is placed around the human body and the other is inserted into the blood vessel in front of the guidewire of catheterizing angiography. The distance between antennas will be measured by calculating the time of arrival and propagation direction, which will be depending on the ultra-wideband frequency, shape, and other specifications. This distance between the antennas includes the human tissue with its different layers, where each layer has certain dielectric properties enabling us to recognize the tissue type. The drawback of this study is the difficulty of manufacturing a small UWB antenna that can be inserted into the human vessels.

3. UWB medical radar for angiography

Many commonly used medical imaging devices for cardiovascular imaging has been found such as X-ray angiography, cardiac MRI, cardiac CT, and cardiac ultrasound (echo). These devices have some limitations such as radiographic exposure,

high cost, high complexity, long time requirement, limited resolution, or other medical preventions. These limitations motivate us to begin this research and attempt to find a new technique that avoids the ionizing radiation as well as minimize the cost and complexity. The ultra-wideband technology with its distinctive specifications is the suitable technique.

3.1 Medical UWB radar methodology

The medical cardiovascular imaging UWB radar is a new approach for medical multi-static radar which depends on the use of two different transceivers. The first transceiver is a horn type that has been built around the body of angiography (encloses the human body), while the other is a micro-strip which has been inserted into the human blood vessel with the angiography guidewire. The wave pulses of medical radar traveled through the human tissues and then arrived at the receiver. According to the high dielectric properties, differences among the human tissues, and the blood, the radar can recognize the blood in the vessels, where the high percentage of water tissues (like blood) has high dielectric properties in comparison with other tissues. Also, the reflection coefficients' amplitude and time of peaks have been affected by the depth of blood vessels, thus making the ultra-wideband radar so favorable for cardiovascular imaging. The formation of the medical image is required for the finding of the distance between the two antennas, the propagation direction (Θ), and the time of arrival (TOA), which will be different from one tissue to another, depending on the dielectric properties (permittivity) of the tissue. The wave pulses passing through tissues with high dielectric properties (like blood) will be faster than when it passes through tissues with low dielectric properties. Also, the layers (tissues) have been recognized, depending on the finding of reflection pulses at the time of arrival and propagation direction.

Figure 4 illustrates the possible scenarios for wave propagation (transmission) through the body layers; these scenarios are explained in the conclusion. The new medical radar has been worked instead of the X-ray angiography. To minimize the biological side effects of X-ray RF, which provides accurate real-time imaging which is necessary at catheterization angiography operation for clear imaging, the new medical radar is designed according to the standard model IEEE 802.15.3a channel parameters that consider a fifth derivative Gaussian pulse ultra-wideband with a frequency center of 5 GHz. These pulses have been passed through a hypothetical medium (which represent the human tissues); this medium has been represented by the additive white Gaussian noise (AWGN) and medium gain with a certain delay, where the delay and propagation direction in real cases will depend on the tissues that are passed through. Finally, the received signal will be compared with the transmitted signal by using a cross-correlator. **Figure 5** illustrates this simulation, which represents the MATLAB simulation for the new medical radar with all proposed components.

3.2 Medical radar equations

UWB waves transmit through the body tissue layers (mediums) under electromagnetic wave propagation laws, where the velocity of waves are different from one to another layer according to the dielectric properties (permittivity) of this medium [34, 37]:

$$\mathbf{Vi} = \frac{c}{\sqrt{\varepsilon i}} \tag{4}$$

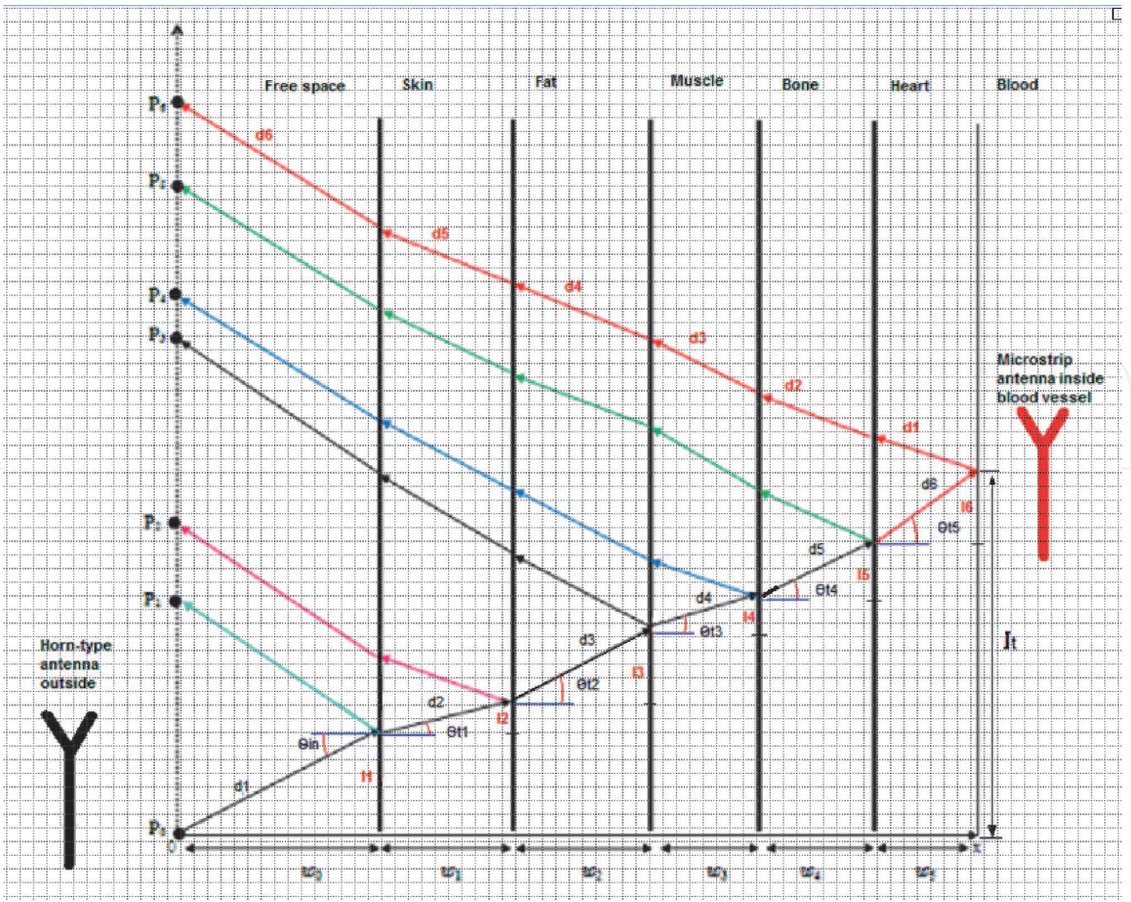

Figure 4.
Distance between two antennas with the including layers.

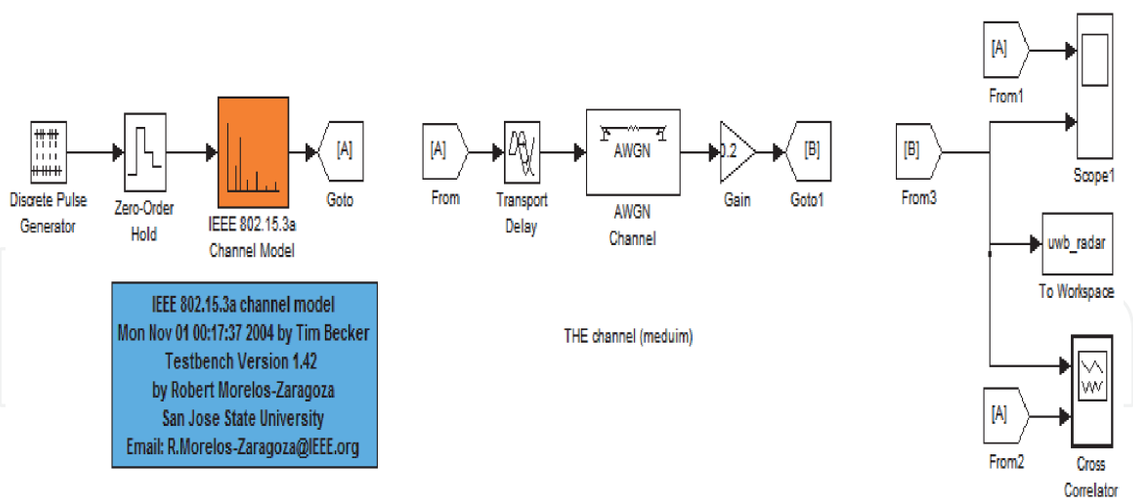

Figure 5.
MATLAB simulation for the proposed UWB medical radar.

where V_i is the velocity in layer i, c is the velocity in free space, and ε_i is the permittivity of the medium. The transmitted angle between two layers will be different from medium to another depending on the intrinsic impedance of the two mediums η_o and η_i and as in **Figure 3** and in [20]:

$$\Theta ti - 1 = sin^{-1}\left(\frac{\eta o}{\eta i}\sin(\Theta in)\right) \quad (5)$$

where Θ_{in} is the incident angle which must be greater than the critical angle [37]:

$$\boldsymbol{\Theta c} = sin^{-1}\left(\sqrt{\frac{\varepsilon i + 1}{\varepsilon i}}\right) \tag{6}$$

Here, Θ_c is founded only if the wave transmits from a denser to a less dense layer. And to find the one-way distance between the two transceivers of our radar, we need to find the one-way distance of each layer individually and the distance for the first layer (d_1), second layer (d_2), and any layer (d_i) as the following [20]:

$$\mathbf{d}1 = \frac{l1}{\sin(\Theta in)} \tag{7}$$

$$\mathbf{d_2} = \mathrm{d}_1 + \frac{l2}{\sin(\Theta t1)} \tag{8}$$

$$\mathbf{d_i} = d_{i-1} + \frac{li}{\sin(\Theta t2)} \tag{9}$$

where l_1, l_2, and l_i are obtained from the following equations:

$$\boldsymbol{l_1} = \mathrm{w}_0 \ \tan(\Theta_{\boldsymbol{in}}) \tag{10}$$

$$\boldsymbol{l_2} = \mathrm{w}_1 \ \tan(\Theta_{\boldsymbol{t1}}) \tag{11}$$

$$\boldsymbol{l_i} = \mathrm{w}_i \ \tan(\Theta_{\boldsymbol{ti-1}}) \tag{12}$$

where ω is the frequency of the wave. The vertical offsets between the two antennas (It) can be obtained by the equation:

$$\boldsymbol{l_t} = \boldsymbol{l_1} + \boldsymbol{l_2} + \boldsymbol{l_3} \ldots . + \boldsymbol{l_i} \tag{13}$$

Also, to find the time $\boldsymbol{t_1}$, $\boldsymbol{t_2}$, and $\boldsymbol{t_i}$ for each layer:

$$\boldsymbol{t_1} = \frac{\boldsymbol{d1}}{\boldsymbol{c}} \tag{14}$$

$$\boldsymbol{t_2} = \boldsymbol{t_1} + \frac{\boldsymbol{d_2} - \boldsymbol{d_1}}{\boldsymbol{v_1}} \tag{15}$$

$$\boldsymbol{t_i} = \boldsymbol{t_{i-1}} + \frac{\boldsymbol{d_i} - \boldsymbol{d_{i-1}}}{\boldsymbol{v_{i-1}}} \tag{16}$$

where Vi is the velocity of wave in the medium. Also, the most important law in our calculations is the intrinsic impedance η for each layer (medium) [38]:

$$\eta = \frac{\sqrt{\mu/\varepsilon}}{\left[\mathbf{1} + \left(\frac{\sigma}{w\varepsilon}\right)^2\right]^{\frac{1}{4}}} \tag{17}$$

where μ is the permeability, Ɛ is the permittivity, Ϭ is the conductivity, and ω is the frequency of wave. Considering the human body tissues as lossy mediums, μ = μo μr, Ɛ = Ɛo Ɛr, Ϭ ≠ 0, where μo is the permeability of free space, μ_r is the relative permeability, ε_o is the permittivity of free space, ε_r is the relative permittivity, and the dielectric properties of free space are: permittivity ε_o = 8.854 x 10^{-12} (F/m), permeability $\mu_o = 4\pi \times 10^{-7}$ (H/m), and conductivity Ϭ = 0 [38]. Finally, there are other parameters that can be obtained from the intrinsic impedance, and

these parameters are reflection (Γ) and transmission (Γ) coefficients between mediums [34, 39]:

$$\Gamma_{1/2} = \frac{\eta_2 - \eta_1}{\eta_2 + \eta_1} \tag{18}$$

$$T_{1/2} = \frac{2\eta_2}{\eta_2 + \eta_1} \tag{19}$$

Finally, the amplitude of transmitted wave (E_x) will decrease (attenuate) exponentially and can be obtained from the equation:

$$E_x = e^{ax} \tag{20}$$

where x is the crossing distance and a is the attenuation coefficient, while the equations of this wave after incidents at the boundary between the two mediums with different dielectric properties will be:

$$E_t = T.E_i \tag{21}$$

$$E_r = \Gamma.E_i \tag{22}$$

where E_i is the incident wave, E_t is the transmitted wave, E_r is the reflected wave, T is the transmission coefficient, and Γ is the reflection coefficient.

The dielectric properties of human body tissue are estimated by Gabriel [40, 41], so the thicknesses of the tissues (layers) in any region of the human body are represented in [42]. The equations above can be applied on the human body layers depending on the characteristic properties of each tissue which are dependent on the transmitted wave frequency.

3.3 Results and discussion

The above equations have been applied on the human body tissues based on the characteristic properties of the tissues which are dependent on the frequency of transmitted wave.

3.3.1 Intrinsic impedance and transmission angle calculation

The transmission angle between the tissues and the intrinsic impedance of human tissues is calculated as shown in **Table 1**, using a frequency center of 5 GHz, the incident angle of π/4, and based on the permittivity and conductivity (dielectric properties) of all tissues. Here, the intrinsic impedance has a directional relationship with the transmitted wave frequency, while the transmission angle has an inverse relationship with the frequency of the transmitted wave, and also it is based on the intrinsic impedance and the incident angle.

The results in **Table 1** are essential for time, distance, and speed calculation, which are essentially for the tissue recognition needed for image reconstruction, as mentioned in Section 3.2.

3.3.2 Distance and time calculations

The velocity, time, and the distance between the two transceivers (one-way distance) have been calculated by using the characteristic properties of human

Tissue type	Conductivity ϭ (S/m)	Permittivity Ɛ (F/m)	Intrinsic impedance η(Ω)	transmission angle Ɵt
Air	1E-20	1	376.734309	
Skin	3.06	35.774	42.7032786	0.24488786
Fat	0.24	5.0291	138.539578	1.17884328
Muscle	4.04	49.54	36.9706969	0.21196925
Bone	0.96	16.05	72.5312559	0.74134990
Heart	4.86	50.27	34.2849767	0.88705125
Blood	5.4	53.95	32.6208079	0.17272680
Lung	3.94	44.859	37.7366007	0.06408701

Table 1.
Dielectric properties of human tissues.

tissues which are listed in **Table 1**. The thickness of these layers (tissues) are taken in the thorax area and ordered as shown in **Figure 4**.

From the results shown in **Table 2**, the variations in the times and speeds for the layers have been observed and are based on the dielectric properties of each layer. These differences will enable the medical image reconstruction depending on the speed of waves in the tissues.

3.3.3 Reflection and transmission coefficient calculation

The reflection coefficient and transmission coefficient with different frequencies are illustrated in **Figures 6** and 7.

From the results which are illustrated in **Figures 6** and 7, note that the reflection and transmission coefficients have a directional relationship with the frequency of a transmitted wave; and from **Figure 6**, note that the blood has the lowest reflection coefficients, which means the ultra-wideband pulses spend shorter time passing through the blood. Also, the transmission coefficient of skin-air is smaller than the transmission coefficient of air-skin, so improving the reflection and transmission coefficients increases the ability of the radar imaging process in any direction either from the inside to the outside transceiver or from the outside to the inside transceiver, as illustrated in **Figure 4**.

The radar can make the two processes together for getting a very clear image, which makes the new radar pass the problems of previous radars, which have been

Tissue type	Thickness	L	Distance	Time	Velocity
Air	50	50	58.76	2E-07	3E+08
Skin	1.3	−0.32	60.1	2.2E-07	5E+07
Fat	9.5	22.98	84.97	4.1E-07	1E+08
Muscle	13.5	−2.91	98.78	7.3E-07	4E+07
Bone	6.6	−6.04	107.7	8.5E-07	7E+07
Heart	5.65	−6.93	117.9	1.1E-06	4E+07
Blood	1.2	0.209	108.9	8.7E-07	4E+07
Lung	5.7	−0.37	123.6	1.2E-06	4E+07

Table 2.
Distance and time between the layers.

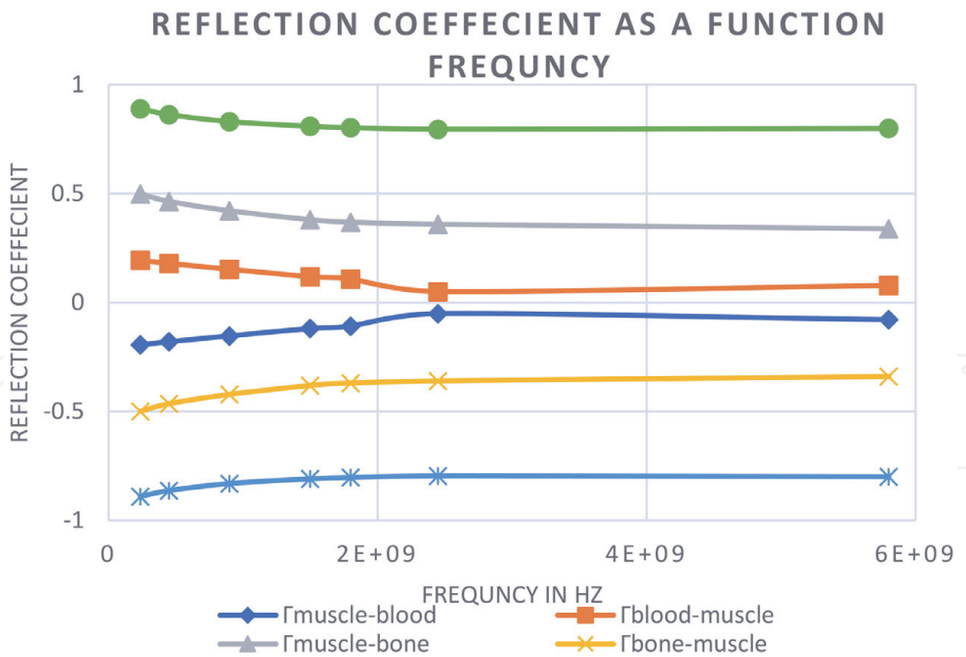

Figure 6.
Relationship between reflection coefficients and frequency.

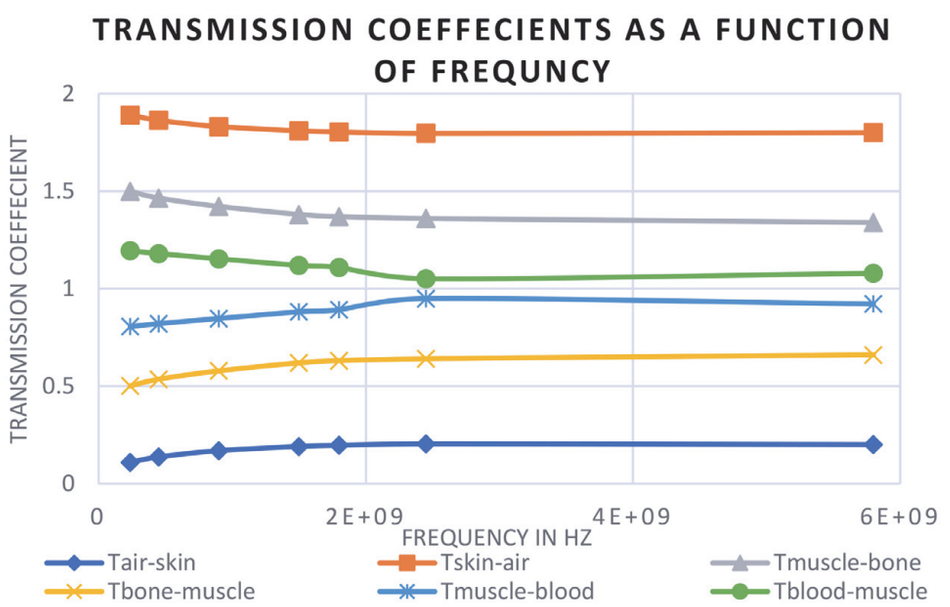

Figure 7.
Relationship between transmission coefficients and frequency.

represented by the power loss in the first layers and the receiving of weak power signals from the other depth layers, also enabling the choosing of the best way that has the lowest reflection coefficient and the highest transmission coefficient due to minimizing of the power dispersion [43].

3.3.4 Experiment results

The first experiment was done by adding the glucose water intravenous nutrient with different concentrations to detect its effects on the dielectric properties of blood (especially on the permittivity), where we will use the glucose concentrations from 70 to 16,000 mg/dL, and **Figure 8** shows the results.

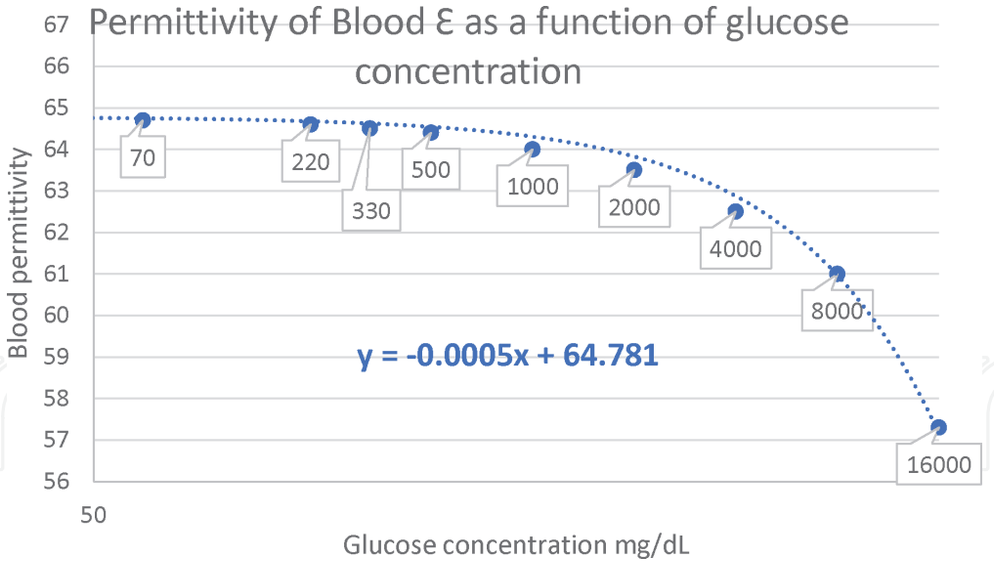

Figure 8.
Permittivity of blood Ɛ as function of glucose concentration.

From the results illustrated in **Figure 8**, the blood permittivity has been decreased gradually when the blood glucose concentration is increased, and the opposite is right, where the blood dielectric properties can be increased by decreasing the blood glucose concentration. Also, these results can be served to design a noninvasive ultra-wideband blood glucose concentration measurement device.

The next experiment has been achieved by adding various normal saline intravenous nutrients' concentration for detecting its effects on the blood dielectric properties (especially the permittivity), where the using of the salinity concentrations from 0 to 2% is applied, and **Figure 9** shows the results. These results have been served to conclude that the blood permittivity will be decreased gradually when the blood salinity percentage, %, is increased, and the opposite is right, where the blood dielectric properties can be increased by decreasing the salinity percentage, %. Also, these results can be served to design a new ultra-wideband device used for detecting the blood salinity percentage noninvasively or for blood pressure measurements.

The last experiment has been achieved by adding the anticoagulant material (citrate or EDTA) to the blood and then measuring its effects on the dielectric properties (permittivity), as illustrated in **Table 3**. From the results above, the adding of anticoagulant to the blood will cause an increase in the blood permittivity.

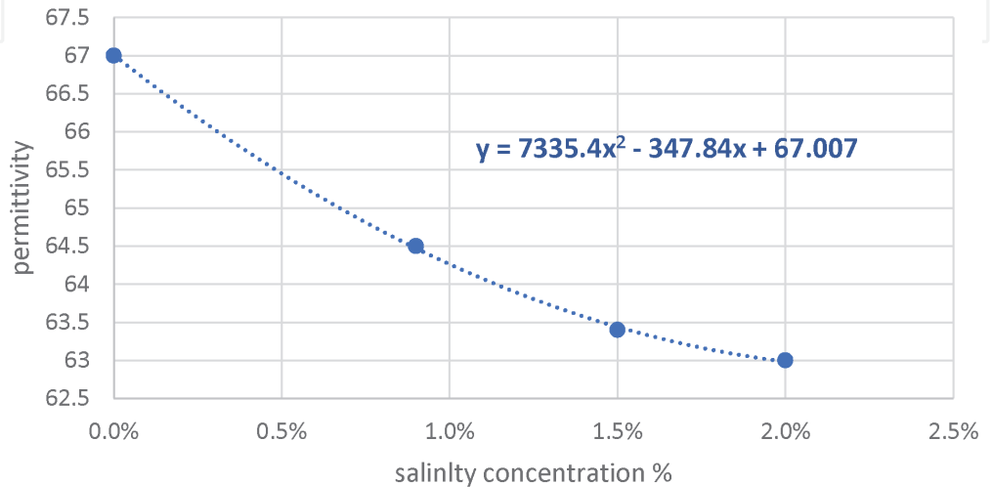

Figure 9.
Permittivity of blood Ɛ as function of salinity concentration.

Pure blood	Blood with citrate	Blood with EDTA
58	62	63.5

Table 3.
Anticoagulant effect.

Note that all experiments have been practiced in the 5 GHz frequency center, with its fitting to the FCC mask, at accepted SAR level, at 37°C temperature, and with fresh blood, and with fresh blood (+O blood group). Also, in the real case, the experiment has some limitations in the adding of these materials to the patients' blood (effected by the patient's condition and his disease background).

4. Ultra-wideband glucometer

It is an ultra-wideband device used for measuring the glucose concentration in the blood noninvasively. The glucose concentration has been found relatively changing within the blood dielectric properties, according to the percentage of glucose that contain. Here, a decrease in the blood dielectric properties (permittivity) has been observed when the glucose percentage was increased (inverse relationship). This decrease was appeared clearly when the frequency range is increased and remained almost constant when it passed the 5GHz as shown as in **Figure 8**. Although, other factors may have an effect on the dielectric properties like temperature, gender, clotting rate, and blood density. This method can be applied accurately by using one ultra-wideband transceiver that is attached to the superficial blood vessel, and then compares the sent and the received signals which have been detected by the same transceiver to calculate the reflection coefficient. The proposed device will be depending on the reflected waves from the blood for measuring the glucose concentration, where a Vivaldi UWB antenna has been attached to the superficial blood vessels to detect the reflection coefficient. The reflection coefficient (Γ) can be obtained from the comparison between the amplitude of transmitted and received (reflected) waves [44]:

$$E_r = \Gamma . E_i \tag{23}$$

where E_i is the incident wave and E_r is the reflected wave. Also, the reflection coefficient has proportional relationship with the blood permittivity (Ɛr) as illustrated below:

$$\Gamma = \frac{\sqrt{\varepsilon_{r1}} - \sqrt{\varepsilon_{r2}}}{\sqrt{\varepsilon_{r1}} + \sqrt{\varepsilon_{r2}}} \tag{24}$$

Finally, the blood glucose concentration has been measured with high percentage of accuracy, which is related to the changes in the blood permittivity (dielectric properties).

5. Conclusions

The finding of the results and hypothesis in Section 3 have concluded a selective direction ultra-wideband imaging radar with multi-static used for angiography with many features; the most important features for this radar are minimizing the power dispersion to the half, which is causing decrease in the attenuation of the signal at

the depth of human tissues, and minimizing the time of arrival (TOA), where the ultra-wideband pulses have been received on the other side where there is no need to pass through human tissue again (one-way). The new radar has been designed to cancel the position calculations of return points, and it just needs to calculate the position of the received antenna on the other side by calculating the total offset (It) which is shown in **Figure 4**. As well as the ability of the new radar, for imaging in both directions (selective direction), makes it avoid the old problems of previous radars with power losses and image collapsing. Also, this new radar can be developed to work with other internal imaging devices like endoscopes and with the alike principle of work and similar design in addition to the study of the ability of improving the radar imaging by injecting the patient's body with a certain substance that manipulates the blood dielectric properties. The finding of the transmission coefficient and reflection coefficient among the multilayer tissue enables the new radar for choosing the best way to the imaging, which has been determined depending on the dielectric properties of tissues under exam. If the ultra-wideband pulses are transmitted from a layer with higher dielectric properties to the next layer with lower dielectric properties, then the reflection coefficient has a negative amplitude and the transmission coefficient has a high positive amplitude according to Eqs. (18) and (19), which will be due to most of the ultra-wideband pulses passing the boundary between the layers and arriving to the next layer, and the little percentage of pulses will be reflected from the boundary and will return in the opposite direction of propagation, and the opposite is right. The experiment results in Section 3.3.4 can introduce additional features that can be used for improving the ultra-wideband imaging through adjusting of the dielectric properties of blood by controlling the reflection and transmission coefficients in accord with the radar requirements. And as mentioned in the above paragraph, if the radar sends pulses from the outer transceiver into the inner one (one-way image), then the transmission coefficient must be improved, while if the radar sends pulses from the outer to another transceiver that is also outside the body (two-way image), then the reflection coefficient must be improved. Finally, the blood dielectric properties can help us to find the glucose concentration noninvasively by using one ultra-wideband transceiver (antenna), depending on the comparison between the transmitted and reflected pulses. The UWB antenna will be attached to the superficial blood vessel to avoid the noise and power attenuation from another human tissue to increase the accuracy of readings (where, the using of two antennas to send and receive the pulses from the other side of the hand will result in the wave being passed through many layers, and the power of the signal will be absorbed, which will cause

Relationship	**Notes**
Glucose concentration $\alpha \frac{1}{\varepsilon}$	
Glucose concentration $\alpha T_{1/2}$	By considering the blood is 2nd medium
Glucose concentration $\alpha T_{1/2}$	By considering the blood is 2nd medium
Anticoagulant material $\alpha \varepsilon$	
Anticoagulant material $\alpha \frac{1}{\Gamma_{1/2}}$	By considering the blood is 2nd medium
Anticoagulant material $\alpha \frac{1}{T_{1/2}}$	By consider the blood is 2nd medium
Blood temperature $\alpha \varepsilon$	
Hemoglobin percentage $\alpha \varepsilon$	

Table 4.
A summary of relationships.

inaccurate measurement). Taking into the account the other parameters can have effects on the dielectric properties, which are mentioned above in Section 1.3. The permittivity has a clear reverse proportional relationship with blood glucose concentration, which can be used to determine the glucose concentration in blood in high accuracy in comparison with the previous studies. **Table 4** will mention a summary of relationships that serve our conclusions:

Author details

Abdulhameed Habeeb Alghanimi
Ministry of Health, Baghdad, Iraq

*Address all correspondence to: abdorck@yahoo.com

References

[1] Federal Communications Commission. Revision of Part 15 of the Commission's Rules Regarding Ultra-Wideband Transmission Systems, First Report and Order. 2010. pp. 02-17

[2] Ahlbom A et al. Guidelines for limiting exposure to time-varying electric, magnetic, and electromagnetic fields (up to 300 GHz). Health Physics. 1998;**74**(4):494-521

[3] Popa A. An optimization of Gaussian UWB pulses. 10th International Conference on Development and Application Systems, Suceava, Romania, May 27-29, 2010; 50

[4] Xie H et al. A varying pulse width 5 th-derivative Gaussian pulse generator for UWB transceivers in CMOS. In: 2008 IEEE Radio and Wireless Symposium. IEEE; 2008. pp. 171-174

[5] Cavagnaro M, Pisa S, Pittella E. Safety aspects of human exposure to ultra wideband radar fields. In: International Symposium on Electromagnetic Compatibility—EMC EUROPE, 17–21 September. 2012. pp. 149-153

[6] Zhang Y, Zhong L, Tan S, Xu C. Dielectric properties of red blood cell suspensions based on broadband dielectric spectrum. In: 2010 IEEE International Conference on Solid Dielectrics. Potsdam, Germany: IEEE. ICSD; 2010. pp. 1-4. DOI: 10.1109/ICSD.2010.5567195

[7] Salahuddin S, Farrugia L, Sammut CV, O'Halloran M, Porter E. Dielectric properties of fresh human blood. In: Proceedings of 2017 19th International Conference on Electromagnetics in Advanced Applications. Ireland, Galway: IEEE. ICEAA; 2017. pp. 356-359. DOI: 10.1109/ICEAA.2017.8065249

[8] Rauf A. A dielectric study on human blood and plasma. **I**nternational Journal of Environmental Science and Technology [Online]. 2013;**2**(6): 1396-1400. Available from: http://www.ijset.net/journal/216.pdf

[9] Salahuddin S, Halloran MO, Porter E, Farrugia L, Bonello J, Sammut CV. Effects of standard coagulant agents on the dielectric properties of fresh human blood. IEEE Transactions on Dielectrics and Electrical Insulation. 2017;**24**(5): 3283-3289. DOI: 10.1109/TDEI.2017.006582

[10] Brodie G, Jacob MV, Farrell P. 6 Techniques for measuring dielectric properties. In: Microwave and Radio-Frequency Technologies in Agriculture. IEEE; 2015. pp. 52-77

[11] Mekhannikov AI, Myl'nikov AV, Maslennikova LP. Calibration of a coaxial antenna-probe for microwave dielectric measurements. Measurement Techniques. 2007;**50**(4):425-428. DOI: 10.1007/s11018-007-0087-2

[12] Cavagnaro M, Pisa S, Pittella E. Safety aspects of human exposure to ultra wideband radar fields. In: International Symposium on Electromagnetic Compatibility—EMC EUROPE. IEEE; 2012. pp. 1-5

[13] Cavagnaro M, Pisa S, Pittella E. Safety aspects of people exposed to ultra wideband radar fields. International Journal of Antennas and Propagation. 2013;**2013**:1-8

[14] Staderini EM. UWB radars in medicine. IEEE Aerospace and Electronic Systems Magazine. 2002; **17**(1):13-18

[15] Paulson CN, Chang JT, Romero CE, Watson J, Pearce FJ, Levin N. Ultra-wideband radar methods and techniques of medical sensing and

imaging. Smart Medical and Biomedical Sensor Technology III. 2005;**6007:** 60070L

[16] Staderini EM, Varotto G. Optimization criteria in the design of medical UWB radars in compliance with the regulatory masks. In: 2007 IEEE Biomedical Circuits and Systems Conference. 2007. pp. 53-58

[17] Leib M, Schmitt E, Gronau A, Dederer J, Schleicher B, Schumacher H. A compact ultra-wideband radar for medical applications. Frequenz. 2009; **63**:1-2

[18] In P. Analysis of vital signs monitoring using an IR-UWB radar. Progress In Electromagnetics Research. 2010;**100**:265-284

[19] Thiel F, Kosch O, Seifert F. Ultra-wideband sensors for improved magnetic resonance imaging, cardiovascular monitoring and tumour diagnostics. Sensors. 2010;**10**(12): 10778-10802. DOI: 10.3390/s101210778

[20] Elmissaoui T, Soudani N, Bouallegue R. New radar system in medicine. In: European Signal Processing Conference. IEEE; 2010. pp. 1640-1644

[21] Jalilvand M, Li X, Zwick T, Wiesbeck W, Pancera E. Hemorrhagic stroke detection via UWB medical imaging. In: Proceedings of the 5th European Conference on Antennas and Propagation (EUCAP). 2011. pp. 2911-2914

[22] Urdaneta M, Wahid P. A study of UWB imaging for bone cancer detection. In: Proceedings of IEEE International Conference on Ultra-Wideband. IEEE; 2012. pp. 197-201. DOI: 10.1109/ICUWB.2012.6340479

[23] Ali MS, Khatun S, Kamarudin LM, Shoumy NJ, Islam M. Non-invasive ultra-wide band system for reliable blood glucose level detection. International Journal of Applied Engineering Research. 2016;**11**(14):8373-8376

[24] Seguin M, Bourqui J, Fear E, Okoniewski M. Monitoring the heart with ultra-wideband microwave signals: Evaluation with a semi-dynamic heart model. Biomedical Physics & Engineering Express. 2016;**2**(3):1-10. DOI: 10.1088/2057-1976/2/3/035011

[25] Mackenberg M, Rackebrandt K, Bollmeyer C. Model Reflection and transmission of ultra-wideband pulses for detection of vascular pressure variation and spatial resolution within soft tissues. Biomedical Physics & Engineering Express. 2016;**2**(2):065003

[26] Yu BG, Oh JH, Kim Y, Kim TW. Accurate measurement of chest compression depth using impulse-radio ultra-wideband sensor on a mattress. PLOS One. 2017;**12**(8):1-8

[27] Alhawari ARH. Lung tumour detection using ultra-wideband microwave imaging approach. Journal of Fundamental and Applied Sciences. 2018;**10**(2):222-234

[28] Der Fang L, Fang WH, Yu LH, Chen YT. Breast tumor detection in the microwave imaging with oblique projection and rao detectors. In: Proceedings of 4th IEEE International Conference on Applied Systems Innovation. Taiwan: IEEE. ICASI; 2018. pp. 239–242. DOI: 10.1109/ ICASI.2018.8394577

[29] Selvaraj V, Baskaran D, Rao PH, Srinivasan P. Breast tissue tumor analysis using wideband antenna and microwave scattering breast tissue tumor analysis using wideband antenna and microwave. IETE Journal of Research. 2018;**01**:1-11. DOI: 10.1080/ 03772063.2018.1531067

[30] Aziz MAI, Rana MM, Islam MA, Inum R. Effective modeling of GBC

based ultra-wideband patch antenna for brain tumor detection. In: International Conferences on Computer, Communication Chemical, Materials and Electronic Enginerring. IC4ME2, Bangladesh: IEEE; 2018. pp. 1-4. DOI: 10.1109/IC4ME2.2018.8465492

[31] Wang L. Electromagnetic sensing and imaging for stroke detection. In: Proceedings of the 2nd International Symposium on Computer Science and Intelligent Control. Sweden: ACM. 2018. pp. 1-6. DOI: 10.1145/3284557.3284734

[32] Lee Y, Park J, Choi Y, Park H, Cho S. A novel non-contact heart rate monitor using impulse-radio ultra-wideband (IR-UWB) radar technology. Scientific Reports. 2018;**8**(1):13053. DOI: 10.1038/s41598-018-31411-8

[33] Shen H et al. Respiration and heartbeat rates measurement based on autocorrelation using IR-UWB Radar. IEEE Transactions on Circuits and Systems II: Express Briefs. 2018;**65**(10): 1470-1474. DOI: 10.1109/TCSII.2018.2860015

[34] Shyu KK, Chiu LJ, Lee PL, Tung TH, Yang SH. Detection of breathing and heart rates in UWB radar sensor data using FVPIEF-based two-layer EEMD. IEEE Sensors Journal. 2019;**19**(2): 774-784. DOI: 10.1109/JSEN.2018.2878607

[35] Alghanimi AH, Fayadh RA. Non-invasive blood glucose measurement depending on the blood dielectric properties by using one ultra-wideband transceiver. International Research Journal of Engineering and Technology. 2019;**06**(07):1494-1498

[36] Alghanimi AH, Fayadh RA. Ultra-wideband radar for angiography. IOP Conference Series: Materials Science and Engineering. 2020;**745**(1). DOI: 10.1088/1757-899X/745/1/012086

[37] Taoufik E, Nabila S, Ridha B. The ultra wide band radar system parameters in medical application. Journal of Electromagnetic Analysis and Applications. 2011;**03**(05):147-154. DOI: 10.4236/jemaa.2011.35024

[38] Sadiku MNO. Elements of Electromagnetics. US: Oxford University Press; 2014

[39] Aardal Ø, Paichard Y, Brovoll S, Berger T. Physical working principles of medical radar. IEEE Transactions on Biomedical Engineering. 2013;**60**(4): 1142-1149

[40] Gabriel S, Lau RW, Gabriel C. The dielectric properties of biological tissues: I. Literature survey. Physics in Medicine and Biology. 1996;**41**:2251-2269

[41] Gabriel S, Lau RW, Gabriel C. The dielectric properties of biological tissues: II. Measurements in the frequency range 10 to 20 GHz. Physics in Medicine and Biology.1996;**41**(11):2251-2269

[42] Christ A, Klingenböck A, Samaras T, Goiceanu C, Kuster N. The dependence of electromagnetic far-field absorption on body tissue composition in the frequency range from 300 MHz to 6 GHz. IEEE Transactions on Microwave Theory and Techniques. 2006;**54**(5):2188-2194. DOI: 10.1109/TMTT.2006.872789

[43] Ketata M, Dhieb M, Chaoui M, Lahiani M, Ghariani H. Electric field attenuation of an ultra wide band wave (UWB) during propagation in the human body. International journal of Sciences and Techniques of Automatic Control & Computer Engineering (IJ-STA). 2010;**4**(1):1188-1197

[44] Pearce FJ, Levin N. Ultra-wideband radar methods and techniques of medical sensing and imaging. Smart Medical and Biomedical Sensor Technology III. 2005;**6007**:60070L